BRAIN COMMUNICATIONS

Interactive effects of HIV and ageing on neural oscillations: independence from neuropsychological performance

Brandon J. Lew,[1] Jennifer O'Neill,[2] Michael T. Rezich,[1] Pamela E. May,[1] Howard S. Fox,[3] Susan Swindells,[2] and Tony W. Wilson[1]

HIV infection is associated with increased age-related co-morbidities including cognitive deficits, leading to hypotheses of HIV-related premature or accelerated ageing. Impairments in selective attention and the underlying neural dynamics have been linked to HIV-associated neurocognitive disorder; however, the effect of ageing in this context is not yet understood. Thus, the current study aimed to identify the interactive effects of ageing and HIV on selective attention processing. A total of 165 participants (92 controls, 73 participants with HIV) performed a visual selective attention task while undergoing magnetoencephalography and were compared cross-sectionally. Spectrally specific oscillatory neural responses during task performance were imaged and linked with selective attention function. Reaction time on the task and regional neural activity were analysed with analysis of covariance (ANCOVA) models aimed at examining the age-by-HIV interaction term. Finally, these metrics were evaluated with respect to clinical measures such as global neuropsychological performance, duration of HIV infection and medication regimen. Reaction time analyses showed a significant HIV-by-age interaction, such that in controls older age was associated with greater susceptibility to attentional interference, while in participants with HIV, such susceptibility was uniformly high regardless of age. In regard to neural activity, theta-specific age-by-HIV interaction effects were found in the prefrontal and posterior parietal cortices. In participants with HIV, neuropsychological performance was associated with susceptibility to attentional interference, while time since HIV diagnosis was associated with parietal activity above and beyond global neuropsychological performance. Finally, current efavirenz therapy was also related to increased parietal interference activity. In conclusion, susceptibility to attentional interference in younger participants with HIV approximated that of older controls, suggesting evidence of HIV-related premature ageing. Neural activity serving attention processing indicated compensatory recruitment of posterior parietal cortex as participants with HIV infection age, which was related to the duration of HIV infection and was independent of neuropsychological performance, suggesting an altered trajectory of neural function.

1 Department of Neurological Sciences, University of Nebraska Medical Center, Omaha, NE, USA
2 Department of Internal Medicine, Division of Infectious Diseases, University of Nebraska Medical Center, Omaha, NE, USA
3 Department of Pharmacology and Experimental Neuroscience, University of Nebraska Medical Center, Omaha, NE, USA

Correspondence to: Tony W. Wilson
University of Nebraska Medical Center
988422 Nebraska Medical Center
Omaha, NE 68198-8422 USA
E-mail: twwilson@unmc.edu

Keywords: HIV; ageing; magnetoencephalography; attention; theta

Abbreviations: cART = combination antiretroviral therapy; HAND = HIV-associated neurocognitive disorder; MEG = magnetoencephalography; PWH = persons with HIV

Received September 18, 2019. Revised December 23, 2019. Accepted January 17, 2020. Advance Access publication February 20, 2020

Graphical Abstract

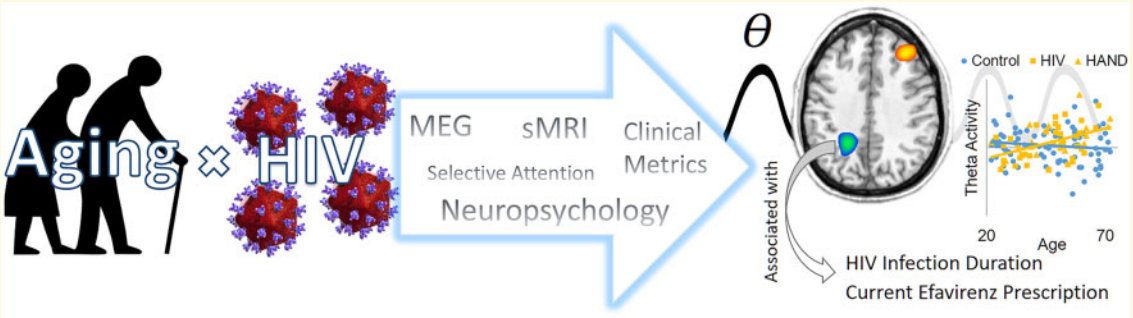

Introduction

The successes of combination antiretroviral therapy (cART) have substantially increased life expectancy in persons with HIV (PWH) who can now expect to live a relatively normal lifespan (Samji *et al.*, 2013). Despite these successes, the impact of ageing in PWH is now a topic of major concern, as these individuals may have heightened susceptibility to co-morbidities associated with ageing (Rodriguez-Penney *et al.*, 2013). Indeed, age-related co-morbidities appear to affect younger PWH more frequently than those who seroconvert at an older age (Guaraldi *et al.*, 2015). These and other findings (Gross *et al.*, 2016) have given rise to hypotheses of premature or accelerated ageing with chronic HIV disease.

Recent research focusing on ageing in HIV has aimed to find biomarkers of accelerated ageing in the brain and/or periphery that can quantify the unique ageing process in PWH (Pathai *et al.*, 2014). Among these studies, neuroimaging investigations of HIV are becoming more sophisticated, with structural and functional alterations linked to HIV infection and ageing (Chang and Shukla, 2018). Early structural MRI studies of PWH naïve to treatment showed brain atrophy indicative of accelerated ageing (Chiang *et al.*, 2007; Wright *et al.*, 2016), and more recent studies in the cART era have tended to support this (Holt *et al.*, 2012; Guha *et al.*, 2016). Conversely, other neuroimaging studies have shown independent effects of HIV and ageing on brain volume (Ances *et al.*, 2012), as well as on cerebral blood flow and brain activation (fMRI; Ances *et al.*, 2010). In this context, magnetoencephalography (MEG) functional imaging is a particularly novel and promising technique for identifying biomarkers of HIV and neural ageing (Wilson *et al.*, 2019). However, despite multiple MEG studies showing HIV-related changes in neural function and dynamics (Wilson *et al.*, 2013*b*, 2017; Wiesman *et al.*, 2018), no studies have examined ageing in HIV.

Another major question surrounds the relationship between premature ageing and incidence of HIV-associated neurocognitive disorder (HAND). HAND is thought to be linked with neuroimmune-related inflammation (Gannon *et al.*, 2011) and while cART has sharply reduced the most severe forms of HAND (i.e., HIV-associated dementia), milder forms remain quite common with estimates ranging from 35% to 70% of all PWH (Simioni *et al.*, 2010; Heaton *et al.*, 2011; Winston *et al.*, 2013; Sacktor *et al.*, 2016). Previous studies have linked accelerated ageing and HAND (Levine *et al.*, 2016; Sheppard *et al.*, 2017), but the relationship between brain ageing and HAND has yet to be fully understood, and the impact of the many other factors at play (e.g. drug misuse and cART neurotoxicity) also needs further study.

In the current study, we aimed to investigate interactions between ageing and HIV-infection on the neural oscillations that serve visual attention function. We hypothesized that selective attention functioning in PWH would follow a differential trajectory of age-related change as compared to adults without HIV. Our overall objective was to examine these differences in the context of neural oscillations and to identify how ageing-related alterations in neural activity were associated with neuropsychological performance and HIV-related clinical measures.

Materials and methods

Participant recruitment

Adults with HIV were recruited from the HIV Clinic of the University of Nebraska Medical Center and demographically matched uninfected control participants were recruited from the local community. To optimize the study of ageing, participants were recruited to create an even distribution across age, ranging from 22 to 72 years. For the HIV-infected groups, inclusion criteria included receiving effective cART and having an undetectable viral load within 3 months of participation in the study, defined as <50 copies/ml. Uninfected controls were recruited to match HIV-infected participants based on their ethnicity, age, sex and handedness. Exclusion criteria included any chronic medical illness affecting CNS function (other than HIV-infection/HAND), any neurological or psychiatric

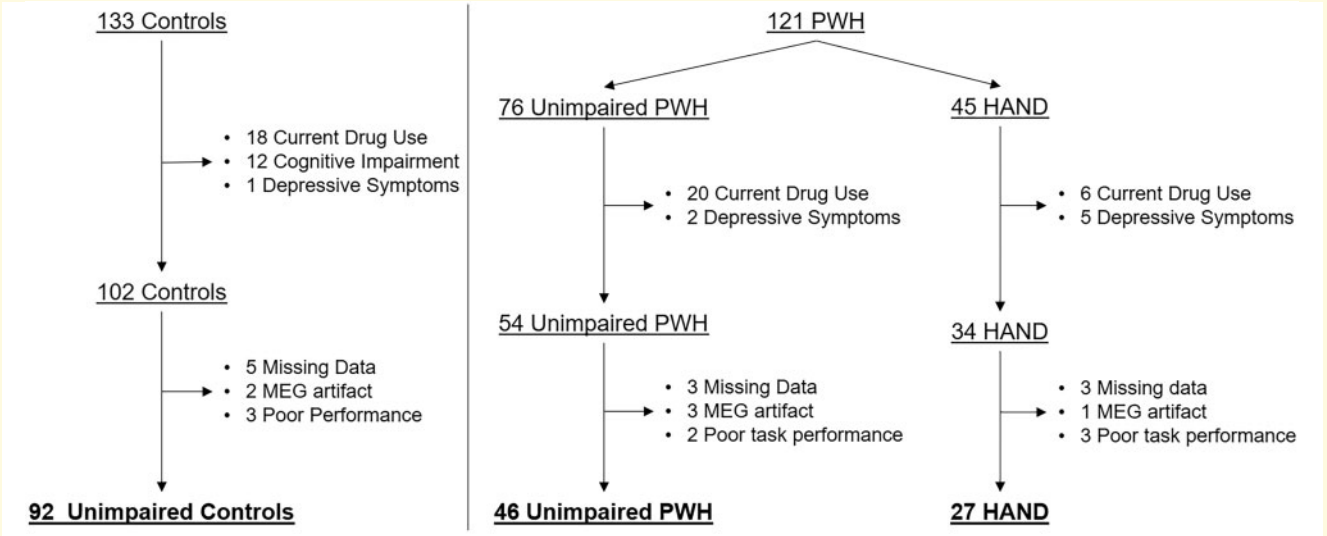

Figure 1 Participant disposition. In total, 133 controls and 121 PWH were enrolled. Participants were excluded for current drug use and moderate-to-severe depressive symptoms. Control participants who were found to be cognitively impaired were also excluded. Finally, participants were excluded due to missing or artefactual MEG data, or poor MEG task performance. The final sample included 92 unimpaired controls, 46 unimpaired PWH and 27 participants with HAND.

disorder (other than HAND), acute intercurrent illness, pregnancy, history of head trauma, current substance use disorder and presence of any ferrous metal implant, including orthodonture, which may interfere with the MEG data acquisition and/or be an MRI safety concern. For this study, additional exclusions of active drug use or alcohol abuse, moderate-to-severe depressive symptoms on the Beck Depression Inventory (Beck *et al.*, 1988) and incomplete or artefactual MEG data were implemented as outlined in Fig. 1. The Institutional Review Board at the University of Nebraska Medical Center approved this protocol. Each participant provided written informed consent, and all participants completed the same protocol.

Neuropsychological battery

This study followed the same protocol as described in Lew *et al.* (2018). Participants completed a neuropsychological battery assessing multiple functional domains, including attention [WAIS-III Symbol Search (Wechsler, 1997) and Stroop Word (Comalli Jr *et al.*, 1962)], speed of processing [Trail Making Part A (Heaton *et al.*, 2004), WAIS-III Digit Symbol, and Stroop color], executive functioning [Trail Making Part B, Stroop interference, phonemic verbal fluency and semantic verbal fluency (Heaton *et al.*, 2004)], fine motor [grooved pegboard (Kløve, 1963; Heaton *et al.*, 2004)], verbal learning and memory [Hopkins Verbal Learning Test–Revised (Benedict *et al.*, 1998)] and language [Wide Range Achievement Test-4th edition (Wilkinson and Robertson, 2006), Word Reading subtest]. Composite scores for each domain were computed by calculating demographically normalized z-scores and taking an average of the z-scores for all tests within that domain. Along with an assessment of activities of daily living, these scores were used to diagnose HAND according to the Frascati guidelines (Antinori *et al.*, 2007). Analyses utilized a full composite score, which represented an average of all neuropsychological composite scores across domains.

MEG acquisition and selective attention task

To examine selective attention and susceptibility to interference, participants completed an arrow-based Eriksen flanker task while undergoing MEG (Eriksen and Eriksen, 1974). Briefly, participants performed 200 trials of the task, each beginning with a fixation that was presented for 1.45–1.55 s, followed by a row of five arrows for 2.50 s. Participants responded with their right hand whether the middle arrow was pointing to the left (index finger) or right (middle finger), and trials were considered congruent when the middle arrow was in the same direction as the flanking arrows, and incongruent when the middle arrow was in the opposite direction. Participants completed the task in a non-magnetic chair in a one-layer magnetically shielded room with active shielding engaged to compensate for environmental noise. Throughout the task, MEG data were collected continuously at 1 kHz with an acquisition bandwidth of 0.1–330 Hz using a 306-sensor Elekta system (Helsinki, Finland). Further details about the flanker task and MEG data acquisition can be found in McDermott *et al.* (2017).

MEG preprocessing, time–frequency transformation and sensor-level statistics

MEG data preprocessing used Brain Electrical Source Analysis software (BESA version 6.1; BESA GmbH, Gräfelfing, Germany) and followed previously published methods described in McDermott *et al.* (2017). Briefly, each participant's data were individually corrected for head movement and subjected to noise reduction using the temporally extended signal space separation method (Taulu and Simola, 2006). Cardiac and blink artefacts were corrected using signal-space projection (SSP; Uusitalo and Ilmoniemi, 1997). MEG data were then divided into epochs of 2.00 s duration (−500 to 1500 ms), with 0.0 s defined as stimulus onset and the baseline defined as the −450 to −50 ms time window. Noisy and high-amplitude trials were rejected based on a participant-specific fixed threshold method as described in Proskovec *et al.* (2018). After artefact rejection, an average of 82.69 trials in the congruent and 81.96 trials in the incongruent condition remained in each participant; and the difference in number of accepted trials did not differ between condition ($t(165)=1.32$, $P>0.10$), nor between groups ($F(2,163)=2.11$, $P>0.10$).

Artefact-free epochs were transformed into the time–frequency domain using complex demodulation at a 1.0 Hz, 50 ms resolution. Specific time–frequency windows of interest were determined by statistical analysis of the sensor-level spectrograms across all correct trials (congruent and incongruent) for each gradiometer in the array. Each data point in the spectrogram was initially evaluated using a mass univariate approach based on the general linear model. To reduce the risk of false-positive results while maintaining reasonable sensitivity, a two-stage procedure was followed to control for Type 1 error. In the first stage, paired-sample *t*-tests comparing each data point to its spectrally respective baseline were conducted and the output spectrogram of *t*-values was thresholded at $P<0.05$ to define time–frequency bins containing potentially significant oscillatory deviations across all participants. In Stage 2, time–frequency bins that survived this threshold were clustered with temporally and/or spectrally neighbouring bins that were also significant, and a cluster value was derived by summing all of the *t*-values of all data points in the cluster. Non-parametric permutation testing was then used to derive a distribution of cluster values and the significance level of the observed clusters (from stage one) was tested directly using this distribution (Ernst, 2004; Maris and Oostenveld, 2007). For each comparison, at least 10 000 permutations were computed to build a distribution of cluster values. Based on these analyses, the time–frequency windows containing significant oscillatory events across all participants and conditions were selected for imaging.

MEG source imaging

Structural T1-weighted MRI images were acquired with a Philips Achieva 3 T X-series scanner using an eight-channel head coil and a 3D fast field echo sequence with the following parameters: TR: 8.09 ms; TE: 3.7 ms; field of view: 24 cm; matrix: 256 × 256; slice thickness: 1 mm with no gap; in-plane resolution: 0.9375 × 0.9375 mm; sense factor: 1.5. Each participant's MEG data were then coregistered with their individual structural T1-weighted MRI data. For the few participants that did not complete an MRI (3% of participants), a template MRI was used. For each statistically determined time–frequency window, the underlying cortical activity was imaged using a reference-free dynamic imaging of coherent sources beamformer (Van Veen *et al.*, 1997; Gross *et al.*, 2001). This approach derives the local power in voxel space by utilizing Fourier-transformed data to calculate the cross-spectral densities of all combinations of MEG gradiometers averaged over the time–frequency range of interest. For the forward solution, we employed a spherical head model and a 4.0 × 4.0 × 4.0 mm voxel space grid with two orientations per voxel. Effectively, the beamformer operator generates a spatial filter for each grid point, which passes signals without attenuation from a given neural region while minimizing interference from activity in all other brain areas. The properties of these filters are determined from the MEG covariance matrix and the forward solution for each grid point in the image space, which are used to allocate sensitivity weights to each sensor in the array for each voxel in the brain. The individual images were normalized using a separately averaged pre-stimulus noise period of equal duration and bandwidth (Hillebrand *et al.*, 2005). Separate images were computed for each condition per time–frequency window in order to optimize the beamformer weighting vectors for each condition (Barratt *et al.*, 2018), and to test for conditional differences. All beamformer images were visually inspected individually for significant outliers, and such images were excluded from whole-brain statistics. We also conducted a *post hoc* analysis to understand the impact, if any, of these exclusions on the final results.

Statistical analysis

The goal of the study was to determine the interactions between age and HIV on selective attention function, both behaviourally and in the brain. Due to the size of the HAND group in comparison to the control group, all primary analyses focused on the comparison between controls and PWH, regardless of HAND status. *Post hoc* analyses were then used to examine whether group differences were independent of, or driven by, neuropsychological impairment. Mixed-model ANCOVA was used to examine reaction time on the task, using condition (congruent versus incongruent) as a within-participants factor, HIV status as a between-participants factor and age as a

covariate of interest. The HIV-by-age interaction term was included to examine the interactive effect of HIV and age, and this term was excluded to probe the lower order interactions (condition-by-HIV and condition-by-age). Additionally, to determine the effect of HAND, we re-ran the analyses after breaking up the HIV group into unimpaired PWH and those with HAND.

To statistically determine the interaction between age and HIV on neural activity, we performed whole-brain ANCOVAs. We first subtracted each participant's congruent image from their incongruent image to obtain flanker 'interference maps'. Statistics on these images effectively test for the condition interaction (i.e. susceptibility to interference) with the variable of interest. We then ran whole-brain ANCOVAs using HIV and age as factors of interest. Finally, a $P < 0.001$ and k threshold of 200 voxels was applied to the resulting map representing the interaction between age and HIV on flanker interference. For each significant cluster, the voxel with the highest F-value was used for regression with clinical metrics.

Effects of HIV-related clinical measures

We also aimed to examine whether our neural findings could be explained by HIV-related clinical measures. These analyses focused exclusively on the PWH. Specifically, we used measures of global neuropsychological performance, duration of HIV infection, current CD4 count, CD4 nadir and current efavirenz-based antiretroviral therapy. We focused on efavirenz because it is known to have CNS-related side effects (Abers *et al.*, 2014). To examine this, we created a categorical variable comparing participants who were currently receiving efavirenz-based cART to those on non-efavirenz regimens. To determine the effects of global neuropsychological performance, we computed an average of the composite scores used to diagnose HAND (see section 'Neuropsychological battery'). We also performed follow-up analyses separating neuropsychological performance by cognitive domain. For duration of HIV infection, we used a self-report measurement of time since diagnosis in years. We then ran univariate ANCOVAs with age, global neuropsychological performance, duration of HIV infection, current CD4 count, CD4 nadir and current efavirenz antiretroviral therapy as independent predictors, and reaction time interference (in milliseconds) and neural interference activity (peak voxel amplitude in pseudo-t's) as dependent variables.

Surface-based morphometry

Finally, a follow-up exploratory analysis was performed to examine the cortical thickness in brain regions identified through the MEG analyses as displaying differential HIV-by-age effects. Participants' high-resolution T1-weighted MRI data were processed using the standard surface-based morphometry pipeline in the CAT12 toolbox (http://dbm.neuro.uni-jena.de/cat/, v12.6, 25 February 2020, date last accessed) at a resolution of 1 mm^3 within SPM12. This method utilizes a projection-based thickness approach to estimate cortical thickness and reconstruct the central surface in one step (Dahnke *et al.*, 2013). Briefly, following tissue segmentation (Ashburner and Friston, 2005) the white matter (WM) distance is estimated, and the local maxima are projected onto other grey matter voxels using a neighbouring relationship described by the WM distance. This method accounts for partial volume correction, sulcal blurring and sulcal asymmetries. Topological defects are corrected based on spherical harmonics (Yotter *et al.*, 2011*a*), and the cortical surface mesh was re-parameterized into a common coordinate system via an algorithm that reduces area distortion (Yotter *et al.*, 2011*b*). Finally, the resulting maps were resampled and smoothed using a 15 mm FWHM Gaussian kernel.

Regions of interest (ROIs) were then created by using the peak voxel coordinates identified from the HIV-by-age maps. Specifically, we used the WFU Pickatlas (v3.0; Maldjian *et al.*, 2003; Maldjian *et al.*, 2004). to generate a 10 mm sphere centred on each peak voxel coordinate identified from MEG interaction maps. These normalized volume masks were transformed into surface template space using the transform provided in CAT12. Cortical thickness values were then extracted per participant by computing the average thickness within each ROI mask. Thus, the values reflected the average cortical thickness within the oscillatory response-based ROI (i.e. the cortical tissue displaying a significant HIV-by-age interaction). Statistical comparisons were then made based on the previous statistical models, using cortical thickness in the ROIs as dependent variables. That is, we ran ANCOVAs with HIV and age as factors of interest, interrogating both the HIV-by-age interaction and the independent main effects.

Data availability

The data that support the findings of this study are available from the corresponding author (T.W.W.), upon reasonable request.

Results

Participant demographics and clinical measures

In total, 121 PWH and 133 uninfected controls, aged 22–72 years, were recruited for the study. Of the 121 PWH, 45 were found to have HAND. We excluded 18 controls and 26 PWH who reported current drug use, most of whom reported cannabis use. Additionally, we excluded one control participant and seven PWH who

had a score indicating moderate-to-severe depressive symptoms on the Beck Depression Inventory (Beck *et al.*, 1996). Of note, eight PWH who were excluded for drug use also had moderate-to-severe depressive symptoms. Finally, we excluded 12 controls who were found to be cognitively impaired on neuropsychological testing. With respect to data acquisition and task performance, 10 controls, 8 unimpaired PWH and 7 participants with HAND were excluded for missing MEG data, artefactual MEG data (e.g. due to dental work), and/or poor task performance during MEG (i.e. <50% accuracy on either condition). Finally, one participant had a viral load of 54 copies/ml and was still included in the analysis. Ultimately, 92 unimpaired controls and 73 PWH, 27 of whom had HAND (Fig. 1) were included in the final sample. Of the participants with HAND, 19 met diagnostic criteria for asymptomatic neurocognitive impairment, 6 for mild neurocognitive disorder, and 2 met criteria for HIV-associated dementia. Group demographics for the final sample are reported in Table 1. The groups ranged in age from 22 to 72 years, with each group closely matched in age and sex (see Table 1). PWH had a median CD4 of 678 cells/mm^3 (range: 102–2617) at the time of enrollment. Median CD4 nadir for all PWH was 232 cells/mm^3 (range: 3–586), and neither current CD4 nor CD4 nadir differed as a function of HAND status ($P > 0.10$).

Behavioural selective attention deficits

An ANCOVA comparing controls to PWH indicated a significant three-way interaction of condition-by-HIV-by-age on reaction time ($F(1,161) = 6.16$; $P = 0.014$; $\eta^2 = 0.037$; Fig. 2). Probing this interaction revealed a significant condition-by-group interaction such that PWH had larger flanker effects (i.e. greater susceptibility to interference; $F(1,162) = 7.12$; $P = 0.008$; $\eta^2 = 0.042$). Additionally, controls showed a significant condition-by-age interaction such that older age was associated with greater susceptibility to interference ($F(1,90) = 9.99$; $P = 0.002$; $\eta^2 = 0.100$). This association with age was not present in PWH ($P > 0.10$). Simple main effects of condition, group and age were all significant such that the incongruent condition, HIV and older age were associated with longer reaction times (all Ps < 0.005). Notably, the three-way interaction was also significant when splitting the HIV group by HAND status, creating three subject groups ($F(2,159) = 3.944$; $P = 0.043$; $\eta^2 = 0.039$). The condition-by-group interaction additionally remained significant such that the HAND participants were the most susceptible to interference ($F(1,161) = 6.63$; $P = 0.002$; $\eta^2 = 0.076$). Pairwise comparisons of the three groups adjusting for age showed a significant difference between the control and HAND groups ($P < 0.001$), and between the unimpaired HIV and HAND groups ($P = 0.017$). The difference between the control and unimpaired PWH groups was trending ($P = 0.082$). Lastly, it should be noted that one participant with HAND had an outlier interference effect (431.61 ms). This participant's data is not displayed in Fig. 2C, but it was included in the analysis, and inclusion/exclusion of the participant's data did not affect the significance of the results.

Susceptibility to interference shows theta-specific HIV-by-age interaction

MEG sensor-level statistics comparing the active and baseline time–frequency windows indicated two distinct spectral windows; one in the theta range (3–6 Hz), and one in the alpha range (8–12 Hz). Briefly, a strong and transient theta synchronization was present from 0 to 350 ms, and a large alpha desynchronization was present from 250 to 700 ms (both cluster $P < 0.001$). These two spectro-temporal windows were used for image reconstruction, with respective baseline periods of equal bandwidth and duration (theta: −400 to −50ms; Alpha: −500ms to −50ms). Images were calculated for congruent and incongruent conditions separately and, to examine interference effects, congruent images were subtracted from incongruent images to generate maps of flanker interference activity.

Whole-brain ANCOVAs examining the interaction between HIV and ageing on flanker interference activity

Table 1 Group demographics

	Controls ($n = 92$)	Unimpaired HIV ($n = 46$)	HAND ($n = 27$)	*P*-value
Age (years)	45.7 (15.7)	47.6 (12.0)	47.5(13.8)	>0.05
Sex (F/M)	41/51	19/27	11/16	>0.05
Race (Caucasian/African American/Other)	66/22/4	34/11/2	15/12/0	>0.05
Average total neuropsychological z-score	0.04 (0.53)	0.01 (0.40)	−0.94 (0.34)	<0.001
Congruent accuracy (%)	98.06 (0.04)	98.72 (0.03)	96.70 (0.07)	>0.05
Incongruent accuracy (%)	98.04 (0.04)	97.98 (0.04)	92.11 (0.14)	<0.001
CD4 nadir in cells/mm^3 (median; range)	–	227 (3–586)	237 (14–469)	>0.05
Current CD4 (median; range)	–	684 (167–2617)	624 (102–1512)	>0.05
Efavirenz-based therapy (# participants)	–	21	10	–

Values are represented as means (SD).

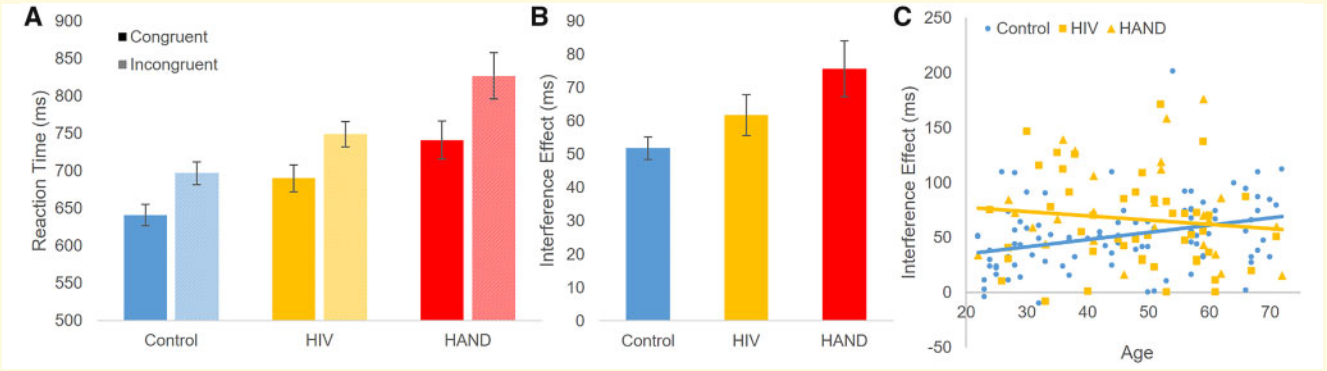

Figure 2 Behavioural performance. (**A**) Mean reaction time per condition and group is shown, with error bars reflecting the SEM. (**B**) The interference effect (incongruent–congruent condition) is shown for each group. (**C**) The susceptibility to interference effect (incongruent minus congruent) is plotted against age for the three groups. Mixed-model ANCOVA revealed a significant condition-by-HIV-by-age interaction and this interaction remained significant when splitting the HIV group by HAND status. For the control group, older age was associated with significantly greater susceptibility to interference. This association was not seen in the HIV group. Instead, the HIV-infected group showed a larger interference effect irrespective of age, largely driven by HAND participants (see **A** and **B**). Overall, this indicates that increased age is associated with increased susceptibility to interference, and that participants with HIV exhibit this effect irrespective of ageing.

were then calculated. With regard to alpha activity, there were no significant HIV-by-age interaction effects. In contrast, for theta, significant interactions were found in the right prefrontal cortex and the left posterior parietal cortex (Fig. 3; $P < 0.001$, corrected). Visualizing these interactions showed that, in the frontal cortex, control participants had a positive relationship between age and interference activity, while PWH had a negative relationship between age and susceptibility to interference (Fig. 3A). In the posterior parietal cortex, controls exhibited no relationship between age and interference activity, while PWH had a positive relationship (Fig. 3B). That is, in the parietal cortex, older PWH showed increasing theta activity with increasing susceptibility to interference. When including all beamformer images regardless of artefacts, similar significant clusters in the prefrontal cortex and posterior parietal cortex were still present. The peak voxels in these statistical interaction maps were then used in correlational analyses between theta interference activity and reaction time interference, but these did not reveal any significant relationships (both P's > 0.10). Additionally, probing the main effects of the theta interference ANCOVA showed a significant effect of HIV in the right inferior parietal cortex, above and beyond age and the HIV-by-age interactive term (Fig. 4). Finally, the main effect of age failed to show any significant clusters.

Neuropsychological performance associated with behavioural performance

Next, we focused on PWH and examined a number of clinical measures. Of note, five PWH did not have current CD4 data, and one participant did not have CD4 nadir data. Additionally, we performed a square root transformation of the current CD4 values to normalize the distribution of data. All other covariates showed normal distributions. An ANCOVA of reaction time interference on age, global neuropsychological performance, duration of HIV infection, current CD4 count, CD4 nadir and current efavirenz-based antiretroviral therapy showed a significant effect of neuropsychological performance above and beyond all other variables ($F(1,60)=13.53$; $P < 0.001$; $\eta^2 = 0.184$), such that poorer global neuropsychological performance was associated with greater behavioural susceptibility to interference. Global neuropsychological performance was the only predictor that was significantly associated with reaction time interference after controlling for all other variables in the model. Notably, global neuropsychological performance was not significantly correlated with any of the clinical measures, including CD4 counts and current efavirenz therapy (all $P > 0.05$). When splitting the global neuropsychological performance variable into its domains and re-running the model, the attention domain was the only domain with a significant effect above and beyond all other variables ($P < 0.05$).

HIV clinical measures associated with parietal theta activity, but not prefrontal activity

To understand the relationship between HIV clinical measures and our identified neural differences, we ran ANCOVA models using the same HIV clinical measures described above as independent variables, and using prefrontal and parietal theta interference activity as dependent variables. As before, these analyses included PWH only. An ANCOVA of theta interference activity in the right prefrontal cortex showed only a significant effect

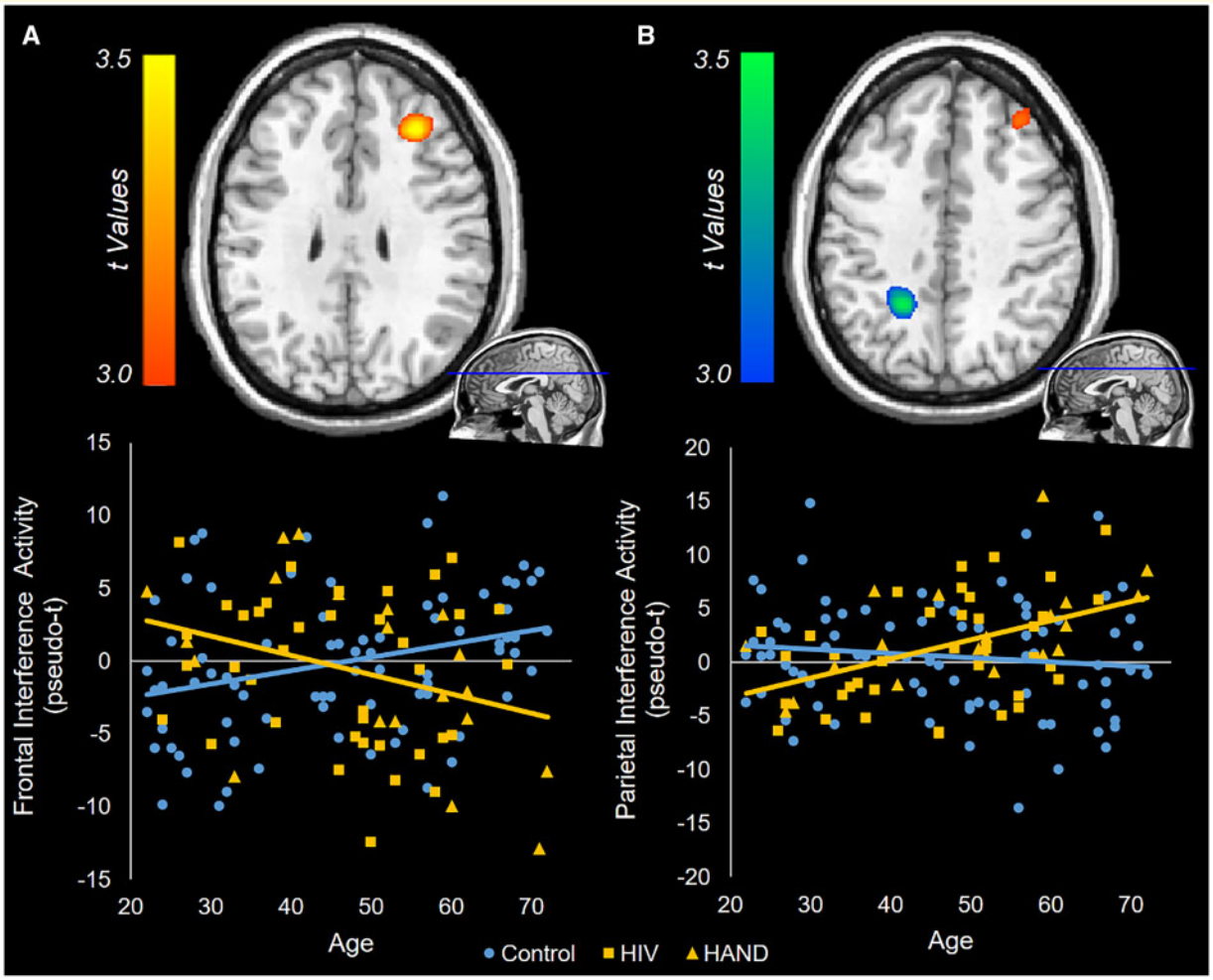

Figure 3 Whole-brain ANCOVAs of theta interference activity. Flanker interference maps were created by subtracting congruent images from incongruent images. These were then subjected to a univariate ANCOVA, and the resulting HIV-by-age interaction contrasts are displayed. Colour bars to the left of each brain image indicate the t-statistic for the age-by-HIV interaction, with warm colours indicating a positive difference between controls and PWH in the age-by-neural activity slope, and cool colours indicating a negative difference. Differences in theta activity were found in the right prefrontal cortex (**A**) and the left posterior parietal cortex (**B**). To visualize these interactions, the peak voxel of each cluster was used to extract the flanker interference values for each participant. Interference activity from the prefrontal peak voxel (**A**) and parietal peak voxel (**B**) was then plotted against age for each group, with HAND participants included in the HIV group, but denoted with yellow triangles (versus yellow squares for unimpaired PWH). Ultimately, in these regions, the relationship between age and flanker interference activity differed as a function of HIV infection.

of age ($F(1,46) = 4.69$; $P = 0.036$; $\eta^2 = 0.092$). In contrast, an ANCOVA of theta interference activity in the left posterior parietal cortex showed significant effects of age ($F(1,46) = 13.18$; $P < 0.001$; $\eta^2 = 0.223$), time since diagnosis ($F(1,46) = 5.34$; $P = 0.025$; $\eta^2 = 0.104$), and current efavirenz-based therapy ($F(1,46) = 8.87$; $P = 0.005$; $\eta^2 = 0.162$), each above and beyond all other predictors. The partial plots and marginal means displaying these significant effects show that older age, longer disease duration and current efavirenz therapy independently predict stronger parietal theta interference activity (Fig. 5). All of these effects also remained significant when including the five individuals missing CD4 data (see above) by using the CD4 count on their medical record closest to their participation in the study. Additionally, these effects remained significant when splitting the global neuropsychology variable into its respective domains, ultimately showing that neither the global nor the individual neuropsychological domains was significant.

Independent effects of HIV and age on cortical thickness

Cortical thickness was computed for all participants with T1 MRIs. ROIs were determined using the prefrontal and parietal peaks displaying significant HIV-by- age interaction effects (Fig. 3). Notably, two participants (both

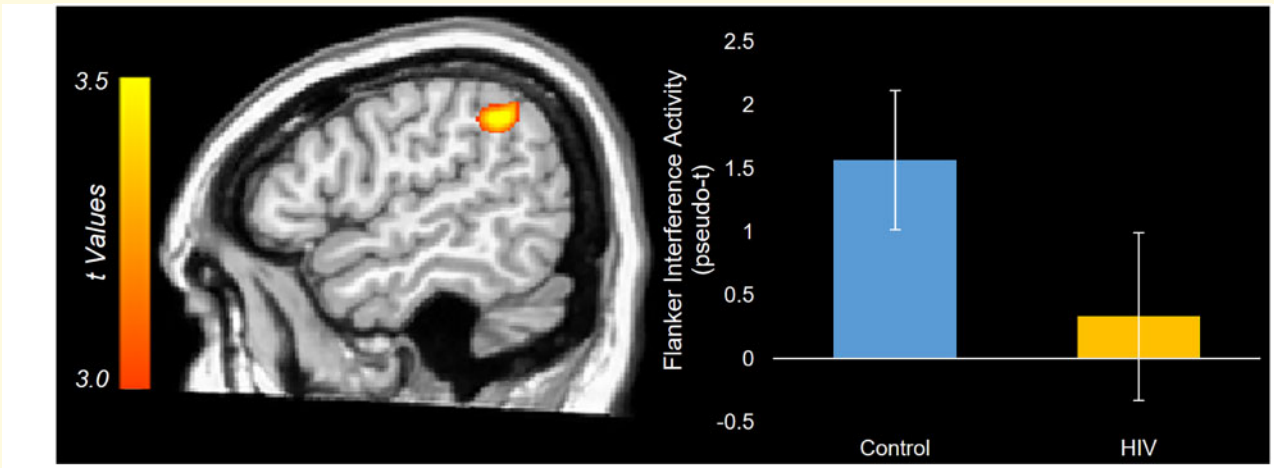

Figure 4 Main effect of HIV on theta interference activity. The theta interference univariate ANCOVA showed a main effect of HIV in the right inferior parietal cortex. The statistical map displaying the main effect of HIV, above and beyond the effects of ageing and their interaction, is displayed with the colour scale bar indicating the *t*-statistic. The peak voxel of the cluster was used to extract the flanker interference values for each participant, and the estimated marginal means for the effect of HIV were then plotted. These values represent the group-wise theta interference activity adjusted for the effect of ageing and the HIV-by-age interaction term. The error bars reflect +/− one SEM.

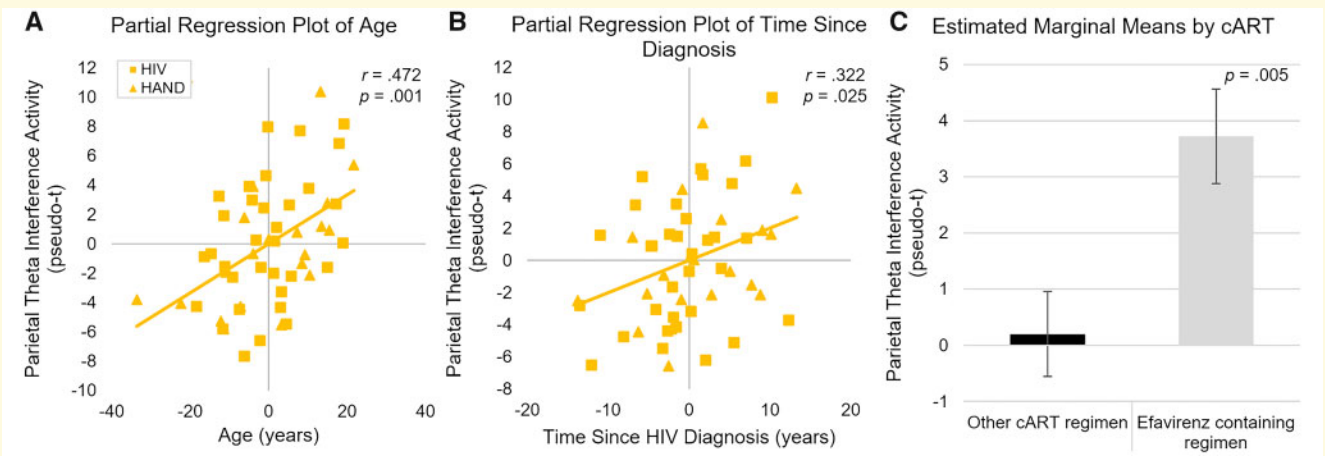

Figure 5 Partial plots of parietal theta interference activity on clinical measures. ANCOVAs of theta activity within the posterior parietal cortex showed that time since diagnosis, age and current efavirenz therapy were significantly associated with interference activity. These predictors were independently significant above and beyond each other, CD4 measures and neuropsychological performance. (**A**) After accounting for other clinical measures, older age was associated with stronger theta interference activity in the parietal. The *Y*-axis shows parietal theta interference activity and the x-axis shows age in years. (**B**) Similarly, time since HIV diagnosis was associated with stronger parietal theta activity; *Y*-axis shows parietal theta interference activity and *X*-axis shows time since HIV diagnosis in years. Participants with HAND were included in these analyses and are shown using triangles. (**C**) Finally, adjusted marginal means for participants currently on cART regimens including efavirenz versus those on other cART regimens showed stronger parietal theta interference activity for those taking efavirenz. Measures in all three plots are shown controlling for all other predictors in the model, and were statistically independent of all other predictors.

PWH) were determined to have low-quality cortical thickness computations when examining sample homogeneity (as defined by >3 SDs away from the mean in overall correlation with other volumes), and thus were excluded from further analyses. Average cortical thickness across the two ROIs (Fig. 6) was determined for each participant and ANCOVAs were utilized to probe the HIV-by-age interaction. These models both failed to show an interaction effect of HIV by age (both P's > 0.10). ANCOVAs without the interactive term were then used to probe the main effects of age and HIV. A main effect of age above and beyond HIV was seen in both the prefrontal ($F(1,155) = 49.66$; $P < 0.001$; $\eta^2 = 0.243$) and parietal ($F(1,155) = 8.27$; $P = 0.005$; $\eta^2 = 0.051$) regions such that

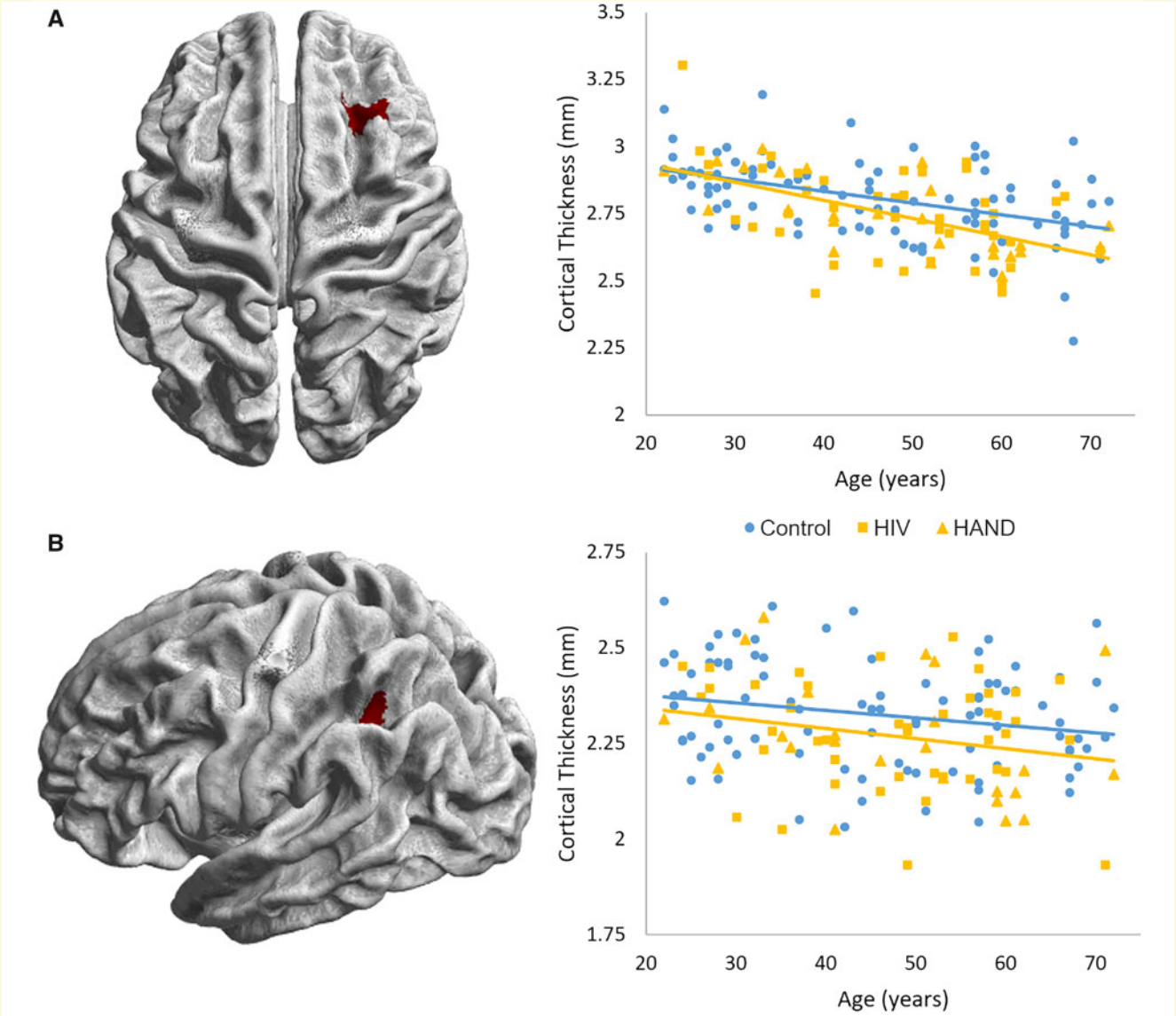

Figure 6 Cortical thickness in prefrontal and parietal regions of interest. Surface-constrained regions of interest were created using the peak voxels of the theta HIV-by-age interaction maps. These masks are displayed with (**A**) corresponding to the right prefrontal peak and (**B**) corresponding to the left parietal peak. The cortical thickness averaged across these ROIs were extracted for each participant, and ANCOVAs were utilized to determine the interaction between HIV and age on cortical thickness. Both regions failed to show an interactive effect of HIV-by-age (both *P*'s > 0.10); however, both ANCOVAs without the interaction term showed main effects of age and HIV above and beyond one another (all *P*'s < 0.05).

increasing age was associated with decreased cortical thickness. Finally, a main effect of HIV above and beyond the effect of age was also found, such that PWH displayed cortical thinning in both prefrontal ($F(1,155) = 5.37$; $P = 0.022$; $\eta^2 = 0.033$) and parietal ($F(1,155) = 5.44$; $P = 0.021$; $\eta^2 = 0.034$) regions (Fig. 6). Bivariate correlations of prefrontal and parietal cortical thickness with their respective theta interference activity did not show significant relationships (both *P*'s > 0.10). When correlating with reaction time interference, decreased left parietal cortical thickness was significantly associated with increased reaction time interference ($r = -0.163$, $P = 0.041$), while prefrontal cortical thickness was not associated with reaction time interference ($P > 0.10$).

Discussion

Our results indicated that selective attention deficits related to HIV infection differ as a function of ageing. Behaviourally, we found that selective attention performance decreases with older age in control participants, while in PWH selective attention was impaired regardless of age. This may be a sign of premature ageing, as

younger PWH appeared to have selective attention abilities near those of much older controls. To examine the neural oscillatory dynamics that underlie this interaction, we ran whole-brain statistics for specific neural responses underlying selective attention processing. These analyses indicated that prefrontal and parietal theta activity had unique relationships with HIV and ageing. Such neural activity did not appear to be related to global neuropsychological performance, potentially showing a pathological ageing process that is independent of HAND. Instead, we found that parietal activity was associated with the duration of HIV infection and current efavirenz therapy. This study is the largest MEG and more broadly the largest functional brain imaging study ever conducted with PWH, and the critical implications for HIV, ageing and cognitive function are discussed at length below.

Our findings of behavioural selective attention deficits in HIV and HAND were consistent with previous literature showing such attention deficits, even in PWH with virologic suppression (Chang *et al.*, 2008; Cysique and Brew, 2009; Wang *et al.*, 2017; Lew *et al.*, 2018). Herein, we extended these findings by identifying how these selective attention deficits change with ageing. The significant association between age and susceptibility to interference in controls suggested that selective attention function normally decreases with age. However, in PWH, our data showed that selective attention deficits were present irrespective of age, which may support the notion of HIV-related premature ageing. In other words, HIV infection may have conferred a selective attention deficit that is normally seen with increasing age, supporting the theory that HIV infection causes premature ageing in the brain. Our data also unsurprisingly showed that global neuropsychological performance is associated with these deficits.

In regards to the MEG data, our findings expand on the growing body of MEG literature focusing on HIV, with HIV-specific differences seen in resting state (Becker *et al.*, 2012, 2013), somato-motor function (Wilson *et al.*, 2013*b*, 2015; Spooner *et al.*, 2018), visual processing (Wilson *et al.*, 2013*a*), working memory (Wilson *et al.*, 2017) and attention (Lew *et al.*, 2018; Wiesman *et al.*, 2018). The current study expands the literature by focusing on ageing in HIV and utilizing a significantly larger sample than any of the previous MEG studies. Whole-brain statistics examining the age-by-HIV interaction revealed two significant clusters in the theta band, one in the right prefrontal cortex and the other in the left posterior parietal cortex. These regions are consistent with recent findings of cortical thickness reductions specifically in frontal and parietal areas in virally suppressed PWH (Sanford *et al.*, 2018). Indeed, we were able to replicate this HIV-related cortical thinning in our ROI analyses, but these structural changes did not show interactive effects with ageing. This lack of an HIV-by-age interaction is consistent with previous structural MRI studies (Cole *et al.*, 2018), and may suggest the effect is more purely functional and/or increased sensitivity of task-based MEG towards such effects. In the left posterior parietal cortex, the interaction effect revealed that older PWH had increased theta activity with greater interference, while control participants showed no relationship between ageing and flanker interference theta activity. This HIV-specific increase in theta power with age may reflect a need for greater recruitment of the parietal cortex during selective attention in older PWH. As per the prefrontal theta activity, PWH had decreasing flanker interference activity with age, while older controls had increasing prefrontal theta activity with increasing age. Together, these data may indicate that, during selective attention processing, controls have a compensatory increase in prefrontal theta with age, while PWH have an aberrant decrease in prefrontal theta recruitment with age and instead exhibit an increase in parietal theta with age. The posterior parietal cortex has specifically been implicated as an essential node in the dorsal attention network, which is critical for top-down attentional control (Ptak and Schnider, 2010). Thus, this compensatory response may be in line with other functional neuroimaging studies of HIV, which have shown greater recruitment of brain reserve networks, specifically during higher attentional demands (Ernst *et al.*, 2002; Chang *et al.*, 2004). Lastly, we also found reduced theta interference activity in PWH relative to controls, irrespective of age, in a more lateral right inferior parietal area that has also been implicated in attention function.

To better understand the clinical importance of these measures, we investigated how our neural findings were associated with HIV-related clinical measures, including global neuropsychological performance, duration of HIV infection, current CD4 count, CD4 nadir and current efavirenz-based antiretroviral therapy. This analysis showed that, in PWH, age remained the only variable that was associated with prefrontal activity above and beyond the other variables. Thus, the mechanism underlying the difference between PWH and controls in the prefrontal cortices remains unclear and definitely warrants further investigation. Greater left parietal activity, on the other hand, was associated with older age, longer time since HIV diagnosis and current efavirenz therapy. It is particularly interesting that each of these measures was independently related to parietal theta activity, controlling for all other variables. This means that, independent of age, the longer an individual has been diagnosed with HIV, the more their parietal activity is aberrant towards that seen in older PWH. This finding may indicate that neural damage associated with HIV is related to the amount of time HIV is present in the brain. Whether this may be better explained by the amount of time patients have a non-zero viral load, or instead continued neural damage despite virologic suppression due to HIV reservoirs in the brain is in need of further study. A pertinent negative finding in this context is that neuropsychological performance was not associated with theta interference

activity in either of these two brain regions. Therefore, participants with HAND did not drive this difference, and the aberrant activity noted here may reflect pathologic brain ageing that is independent of HAND. While HIV-related premature ageing and HAND may be related to one another, our data suggest that the two are not mutually exclusive.

Interestingly, greater left parietal interference activity was also seen for PWH who are currently taking efavirenz. Efavirenz is well known to cause neurologic side effects including dizziness, mood changes and vivid dreams (Abers *et al.*, 2014). Some studies have also linked efavirenz to neurocognitive deficits (Ciccarelli *et al.*, 2011; Ma *et al.*, 2016), although others have shown no neuropsychological differences (Clifford *et al.*, 2005). Our findings appear to link efavirenz to aberrant left parietal theta activity, which may be consistent with studies showing the neurotoxic effects of efavirenz (Apostolova *et al.*, 2017; Ciavatta *et al.*, 2017). However, we did not find differences in global neuropsychological performance linked to current efavirenz therapy, which may indicate a neurotoxic process independent from neuropsychological performance, or at least beyond the functions tapped by our neuropsychological battery.

This study had several limitations. First, the exclusion of majority of participants from the full sample was due to current drug use, specifically cannabis use. While such exclusions help reduce confounds when examining the interaction between HIV and age, cannabis use is more prevalent in PWH (Mimiaga *et al.*, 2013) and therefore further study of this sub-population is important for generalizabilty. Along similar lines, our findings do not extend to individuals with moderate-to-severe depressive symptoms or other psychiatric co-morbidities, as such participants were excluded. Our findings also represent changes seen in virally suppressed PWH and may not extend to those with uncontrolled viraemia. Lastly, the neuropsychological battery administered was brief in nature, perhaps limiting variability in performance globally, and by individual cognitive domains.

In summary, we found that both behavioural and neural measures of selective attention function showed distinct relationships with ageing depending on serostatus. Our behavioural findings may support the notion of HIV-related premature ageing and be related to neuropsychological performance, while our neural findings may reflect HIV-related premature ageing that is independent of global neuropsychological performance. To our knowledge, this study is the largest functional neuroimaging study of HIV and the first to identify altered neural oscillatory activity in the context of HIV and ageing. These findings provide critical new data to aid in our understanding of the relationship between age, HIV and neuropsychological impairment, especially regarding the aberrant neural activity that underlies HIV-related neurologic impairment.

Acknowledgements

We thank the participants and all the study staff. We also acknowledge the enormous contribution from Kevin R. Robertson, PhD, professor of neurology and director of the AIDS Neurological Center at the University of North Carolina at Chapel Hill. Dr. Robertson designed and analysed all the neuropsychological testing, and sadly died during the conduct of the study.

Funding

This research was supported by the National Institutes of Health (NIH; MH103220, MH116782, MH118013, MH062261, DA047828, and DA048713) and the National Science Foundation (NSF: #1539067).

Competing interests

Dr. Swindells reports research grants to her institution from ViiV Healthcare.

References

Abers MS, Shandera WX, Kass JS. Neurological and psychiatric adverse effects of antiretroviral drugs. CNS Drugs 2014; 28: 131–45.

Ances BM, Ortega M, Vaida F, Heaps J, Paul R. Independent effects of HIV, aging, and HAART on brain volumetric measures. J Acquir Immune Defic Syndr 2012; 59: 469–77.

Ances BM, Vaida F, Yeh MJ, Liang CL, Buxton RB, Letendre S, et al. HIV infection and aging independently affect brain function as measured by functional magnetic resonance imaging. J Infect Dis 2010; 201: 336–40.

Antinori A, Arendt G, Becker JT, Brew BJ, Byrd DA, Cherner M, et al. Updated research nosology for HIV-associated neurocognitive disorders. Neurology 2007; 69: 1789–99.

Apostolova N, Blas-Garcia A, Galindo MJ, Esplugues JV. Efavirenz: what is known about the cellular mechanisms responsible for its adverse effects. Eur J Pharmacol 2017; 812: 163–73.

Ashburner J, Friston KJ. Unified segmentation. Neuroimage 2005; 26: 839–51.

Barratt EL, Francis ST, Morris PG, Brookes MJ. Mapping the topological organisation of beta oscillations in motor cortex using MEG. Neuroimage 2018; 181: 831–44.

Beck AT, Steer RA, Brown GK. Beck depression inventory-II. San Antonio 1996; 78: 490–8.

Beck AT, Steer RA, Carbin MG. Psychometric properties of the Beck Depression Inventory: twenty-five years of evaluation. Clin Psychol Rev 1988; 8: 77–100.

Becker JT, Bajo R, Fabrizio M, Sudre G, Cuesta P, Aizenstein HJ, et al. Functional connectivity measured with magnetoencephalography identifies persons with HIV disease. Brain Imaging Behav 2012; 6: 366–73.

Becker KM, Heinrichs-Graham E, Fox HS, Robertson KR, Sandkovsky U, O'Neill J, et al. Decreased MEG beta oscillations in HIV-infected older adults during the resting state. J Neurovirol 2013; 19: 586–94.

Benedict RH, Schretlen D, Groninger L, Brandt J. Hopkins Verbal Learning Test–Revised: normative data and analysis of inter-form and test-retest reliability. Clin Neuropsychol 1998; 12: 43–55.

Chang L, Shukla DK, Imaging studies of the HIV-infected brain. In: Handbook of clinical neurology. Elsevier; 2018. p. 229–64.

Chang L, Tomasi D, Yakupov R, Lozar C, Arnold S, Caparelli E, et al. Adaptation of the attention network in human immunodeficiency virus brain injury. Ann Neurol 2004; 56: 259–72.

Chang L, Yakupov R, Nakama H, Stokes B, Ernst T. Antiretroviral treatment is associated with increased attentional load-dependent brain activation in HIV patients. J Neuroimmune Pharmacol 2008; 3: 95–104.

Chiang M-C, Dutton RA, Hayashi KM, Lopez OL, Aizenstein HJ, Toga AW, et al. 3D pattern of brain atrophy in HIV/AIDS visualized using tensor-based morphometry. Neuroimage 2007; 34: 44–60.

Ciavatta VT, Bichler EK, Speigel IA, Elder CC, Teng SL, Tyor WR, et al. In vitro and ex vivo neurotoxic effects of efavirenz are greater than those of other common antiretrovirals. Neurochem Res 2017; 42: 3220–32.

Ciccarelli N, Fabbiani M, Di Giambenedetto S, Fanti I, Baldonero E, Bracciale L, et al. Efavirenz associated with cognitive disorders in otherwise asymptomatic HIV-infected patients. Neurology 2011; 76: 1403–9.

Clifford DB, Evans S, Yang Y, Acosta EP, Goodkin K, Tashima K, et al., for the A5097s Study Team*. Impact of efavirenz on neuropsychological performance and symptoms in HIV-infected individuals. Ann Intern Med 2005; 143: 714–21.

Cole JH, Caan MWA, Underwood J, De Francesco D, van Zoest RA, Wit F, et al., Comorbidity in Relations to AIDS (COBRA) Collaboration. No evidence for accelerated aging-related brain pathology in treated human immunodeficiency virus: longitudinal neuroimaging results from the comorbidity in relation to AIDS (COBRA) Project. Clin Infect Dis 2018; 66: 1899–909.

Comalli PE, Jr, Wapner S, Werner H. Interference effects of Stroop color-word test in childhood, adulthood, and aging. J Genet Psychol 1962; 100: 47–53.

Cysique LA, Brew BJ. Neuropsychological functioning and antiretroviral treatment in HIV/AIDS: a review. Neuropsychol Rev 2009; 19: 169–85.

Dahnke R, Yotter RA, Gaser C. Cortical thickness and central surface estimation. Neuroimage 2013; 65: 336–48.

Eriksen BA, Eriksen CW. Effects of noise letters upon the identification of a target letter in a nonsearch task. Atten Percept Psychophys 1974; 16: 143–9.

Ernst MD. Permutation methods: a basis for exact inference. Statist Sci 2004; 19: 676–85.

Ernst T, Chang L, Jovicich J, Ames N, Arnold S. Abnormal brain activation on functional MRI in cognitively asymptomatic HIV patients. Neurology 2002; 59: 1343–9.

Gannon P, Khan MZ, Kolson DL. Current understanding of HIV-associated neurocognitive disorders pathogenesis. Curr Opin Neurol 2011; 24: 275–83.

Gross AM, Jaeger PA, Kreisberg JF, Licon K, Jepsen KL, Khosroheidari M, et al. Methylome-wide analysis of chronic HIV infection reveals five-year increase in biological age and epigenetic targeting of HLA. Mol Cell 2016; 62: 157–68.

Gross J, Kujala J, Hamalainen M, Timmermann L, Schnitzler A, Salmelin R. Dynamic imaging of coherent sources: studying neural interactions in the human brain. Proc Natl Acad Sci U S A 2001; 98: 694–9.

Guaraldi G, Zona S, Brothers TD, Carli F, Stentarelli C, Dolci G, et al. Aging with HIV vs. HIV seroconversion at older age: a diverse population with distinct comorbidity profiles. PLoS One 2015; 10: e0118531.

Guha A, Brier MR, Ortega M, Westerhaus E, Nelson B, Ances BM. Topographies of cortical and subcortical volume loss in HIV and aging in the cART era. J Acquir Immune Defic Syndr (1999) 2016; 73: 374–83.

Heaton R, Miller S, Taylor MJ, Grant I. Revised comprehensive norms for an expanded Halstead-Reitan battery: demographically adjusted neuropsychological norms for African American and Caucasian adults. Lutz, FL: Psychological Assessment Resources; 2004.

Heaton RK, Franklin DR, Ellis RJ, McCutchan JA, Letendre SL, Leblanc S, et al., for the CHARTER and HNRC Groups. HIV-associated neurocognitive disorders before and during the era of combination antiretroviral therapy: differences in rates, nature, and predictors. J Neurovirol 2011; 17: 3–16.

Hillebrand A, Singh KD, Holliday IE, Furlong PL, Barnes GR. A new approach to neuroimaging with magnetoencephalography. Hum Brain Mapp 2005; 25: 199–211.

Holt JL, Kraft-Terry SD, Chang L. Neuroimaging studies of the aging HIV-1-infected brain. J Neurovirol 2012; 18: 291–302.

Kløve H, Grooved pegboard. Lafayette, IN: Lafayette Instruments; 1963.

Levine AJ, Quach A, Moore DJ, Achim CL, Soontornniyomkij V, Masliah E, et al. Accelerated epigenetic aging in brain is associated with pre-mortem HIV-associated neurocognitive disorders. J Neurovirol 2016; 22: 366–75.

Lew BJ, McDermott TJ, Wiesman AI, O'Neill J, Mills MS, Robertson KR, et al. Neural dynamics of selective attention deficits in HIV-associated neurocognitive disorder. Neurology 2018; 91: e1860–e9.

Ma Q, Vaida F, Wong J, Sanders CA, Kao YT, Croteau D, et al., for the CHARTER Group. Long-term efavirenz use is associated with worse neurocognitive functioning in HIV-infected patients. J Neurovirol 2016; 22: 170–8.

Maldjian JA, Laurienti PJ, Burdette JH. Precentral gyrus discrepancy in electronic versions of the Talairach atlas. Neuroimage 2004; 21: 450–5.

Maldjian JA, Laurienti PJ, Kraft RA, Burdette JH. An automated method for neuroanatomic and cytoarchitectonic atlas-based interrogation of fMRI data sets. Neuroimage 2003; 19: 1233–9.

Maris E, Oostenveld R. Nonparametric statistical testing of EEG- and MEG-data. J Neurosci Methods 2007; 164: 177–90.

McDermott TJ, Wiesman AI, Proskovec AL, Heinrichs-Graham E, Wilson TW. Spatiotemporal oscillatory dynamics of visual selective attention during a flanker task. Neuroimage 2017; 156: 277–85.

Mimiaga MJ, Reisner SL, Grasso C, Crane HM, Safren SA, Kitahata MM, et al. Substance use among HIV-infected patients engaged in primary care in the United States: findings from the Centers for AIDS Research Network of Integrated Clinical Systems cohort. Am J Public Health 2013; 103: 1457–67.

Pathai S, Bajillan H, Landay AL, High KP. Is HIV a model of accelerated or accentuated aging? J Gerontol A Biol Sci Med Sci 2014; 69: 833–42.

Proskovec AL, Heinrichs-Graham E, Wiesman AI, McDermott TJ, Wilson TW. Oscillatory dynamics in the dorsal and ventral attention networks during the reorienting of attention. Hum Brain Mapp 2018; 39: 2177–90.

Ptak R, Schnider A. The dorsal attention network mediates orienting toward behaviorally relevant stimuli in spatial neglect. J Neurosci 2010; 30: 12557–65.

Rodriguez-Penney AT, Iudicello JE, Riggs PK, Doyle K, Ellis RJ, Letendre SL, et al. Co-morbidities in persons infected with HIV: increased burden with older age and negative effects on health-related quality of life. AIDS Patient Care STDS 2013; 27: 5–16.

Sacktor N, Skolasky RL, Seaberg E, Munro C, Becker JT, Martin E, et al. Prevalence of HIV-associated neurocognitive disorders in the Multicenter AIDS Cohort Study. Neurology 2016; 86: 334–40.

Samji H, Cescon A, Hogg RS, Modur SP, Althoff KN, Buchacz K, et al., for The North American AIDS Cohort Collaboration on Research and Design (NA-ACCORD) of IeDEA. Closing the gap: increases in life expectancy among treated HIV-positive individuals in the United States and Canada. PLoS One 2013; 8: e81355.

Sanford R, Fellows LK, Ances BM, Collins DL. Association of brain structure changes and cognitive function with combination antiretroviral therapy in HIV-positive individuals. JAMA Neurol 2018; 75: 72–9.

Sheppard DP, Iudicello JE, Morgan EE, Kamat R, Clark LR, Avci G, et al. Accelerated and accentuated neurocognitive aging in HIV infection. J Neurovirol 2017; 23: 492–500.

Simioni S, Cavassini M, Annoni JM, Rimbault Abraham A, Bourquin I, Schiffer V, et al. Cognitive dysfunction in HIV patients despite long-standing suppression of viremia. AIDS 2010; 24: 1243–50.

Spooner RK, Wiesman AI, Mills MS, O'Neill J, Robertson KR, Fox HS, et al. Aberrant oscillatory dynamics during somatosensory processing in HIV-infected adults. NeuroImage Clin 2018; 20: 85–91.

Taulu S, Simola J. Spatiotemporal signal space separation method for rejecting nearby interference in MEG measurements. Phys Med Biol 2006; 51: 1759–68.

Uusitalo MA, Ilmoniemi RJ. Signal-space projection method for separating MEG or EEG into components. Med Biol Eng Comput 1997; 35: 135–40.

Van Veen BD, Van Drongelen W, Yuchtman M, Suzuki A. Localization of brain electrical activity via linearly constrained minimum variance spatial filtering. IEEE Trans Biomed Eng 1997; 44: 867–80.

Wang YQ, Pan Y, Zhu S, Wang YG, Shen ZH, Wang K. Selective impairments of alerting and executive control in HIV-infected patients: evidence from attention network test. Behav Brain Funct 2017; 13: 11.

Wechsler D. The Wechsler Memory Scale. San Antonio, TX: Psychological Corp. Harcourt; 1997.

Wiesman AI, O'neill J, Mills MS, Robertson KR, Fox HS, Swindells S, et al. Aberrant occipital dynamics differentiate HIV-infected patients with and without cognitive impairment. Brain 2018; 141: 1678–90.

Wilkinson GS, Robertson GJ. WRAT 4: wide range achievement test. Lutz, FL: Psychological Assessment Resources; 2006.

Wilson TW, Fox HS, Robertson KR, Sandkovsky U, O'Neill J, Heinrichs-Graham E, et al. Abnormal MEG oscillatory activity during visual processing in the prefrontal cortices and frontal eye-fields of the aging HIV brain. PLoS One 2013; 8: e66241.

Wilson TW, Heinrichs-Graham E, Robertson KR, Sandkovsky U, O'Neill J, Knott NL, et al. Functional brain abnormalities during finger-tapping in HIV-infected older adults: a magnetoencephalography study. J Neuroimmune Pharmacol 2013; 8: 965–74.

Wilson TW, Heinrichs -Graham E, Becker KM, Aloi J, Robertson KR, Sandkovsky U, et al. Multimodal neuroimaging evidence of alterations in cortical structure and function in HIV-infected older adults. Hum Brain Mapp 2015; 36: 897–910.

Wilson TW, Lew BJ, Spooner RK, Rezich MT, Wiesman AI. Aberrant brain dynamics in neuroHIV: evidence from magnetoencephalographic (MEG) imaging. Elsevier BV: Progress in Molecular Biology and Translational Science; 2019.

Wilson TW, Proskovec AL, Heinrichs-Graham E, O'Neill J, Robertson KR, Fox HS, et al. Aberrant neuronal dynamics during working memory operations in the aging HIV-infected brain. Sci Rep 2017; 7: 41568.

Winston A, Arenas-Pinto A, Stöhr W, Fisher M, Orkin CM, Aderogba K, et al., for the PIVOT Trial Team. Neurocognitive function in HIV infected patients on antiretroviral therapy. PloS One 2013; 8: e61949.

Wright PW, Pyakurel A, Vaida FF, Price RW, Lee E, Peterson J, et al. Putamen volume and its clinical and neurological correlates in primary HIV infection. AIDS (London, England) 2016; 30: 1789–94.

Yotter RA, Dahnke R, Thompson PM, Gaser C. Topological correction of brain surface meshes using spherical harmonics. Hum Brain Mapp 2011; 32: 1109–24.

Yotter RA, Thompson PM, Gaser C. Algorithms to improve the reparameterization of spherical mappings of brain surface meshes. J Neuroimaging 2011; 21: e134–47.